Journal of Engineering and Sustainable Development
http://jeasd.uomustansiriyah.edu.iq
https://doi.org/10.31272/jeasd.25.1.4

JEASD

Vol. 25, No. 01, January 2021
ISSN 2520-0917

DUCTILITY OF NORMAL AND HIGH STRENGTH CONTINUOUS BEAMS REINFORCED WITH GFRP REBARS

Muayad M. Abdullah[1] ***Hassan F. Hassan[1]**

1) Civil Engineering Department, Mustansiriyah University, Baghdad, Iraq

Received 5/7/2020 ***Accepted in revised form 23/8/2020*** ***Published 1/1/2021***

Abstract: In the reinforced concrete structures, fiber reinforced polymer (FRP) has been considered an alternative material to steel reinforcement with advantages of corrosion resistance, non-conductivity and a high strength to weight ratio. This work is devoted to study the flexural behavior of normal and high strength concrete continuous beams reinforced with glass fiber reinforced polymers (GFRP) rebars. Ten continuous beams, with dimensions 150 mm wide × 250 mm deep × 2300 mm length consisting of two equal span were investigated. The beams were divided into three groups according to the compressive strength of concrete (30, 50 and 70) MPa. Each group consists of three beams with different longitudinal ρ_f (ρ_{fmin}, ρ_{fb} and $1.5\rho_{fb}$; where ρ_{fmin} and ρ_{fb} are the reinforcement ratio at minimum and balanced condition, respectively). Failure load, mid-span deflection, mid-span concrete strains, GFRP reinforcement strains, crack width and ductility of the tested beams were verified and been compared. The experimental results indicate that the increase in the longitudinal ρf increases the failure load by 125% and decreases the crack width and mid-span deflection by 78% and 57%, respectively.

Keywords: *Flexural Behavior*, *Continuous Beams*, *GFRP Rebars*, *Crack Size*, *Ductility*

1. Introduction

Studies and practical for decades of allowed fiber-reinforced polymers (FRPs) to become a particularly actual steel substitute while avoiding problems of corrosion due to their different benefits compared to the conventional materials like high tensile strength, low self-weight, ease of use, easy repairs and even in rather tough environments high durability [1-3]. Carbon, glass, and aramid are the most common types of fibers. GFRP rebars have linear (σ-ε) relationship under stress up to collapse; although, they have lesser elasticity modules and no ductility such as steel rebars, GFRP rebars were used in a developing number of applications due to their higher performance at a reasonably inexpensive cost[4-7]. The flexural behavior of simply supported FRP rebars reinforced concrete members experimentally studied by a many of studies, Rebars is et al. [8] tested twelve simply supported beams reinforced by GFRP rebars, the main variables were longitudinal ρ_f and effective depth-to-height ratios, all beams demonstrated a concrete crushing mode of collapse with final load 51% than expected according to ACI 440.1R-06 [9], also a High degree of deformability was achieved before collapse . Yinghao and Yong [10] studied the flexural behavior of high strength simply supported concrete beams reinforced with

* *Corresponding Author:* hassanfalah@uomustansiriyah.edu.iq

hybrid steel reinforcements and (GFRP), the arrangement of reinforcement layers was the main parameters considered, the use of reinforcement rebars (GFRP - Steel) in the form of a single layer is more effect on final moment capacity than the other arrangements, deflection and cracks size of hybrid beams is greatly affected by the depth of the steel layer. Adam et al. [11] presented an experimental and theoretical study of the flexural behavior of concrete beams reinforced with locally produced (GFRP) rebars, the main parameters were reinforcement material type (GFRP and steel), concrete compressive strength and ρf, the test results showed that, by increasing the ρf, the crack sizes and mid-span deflection were reduced significantly, the collapse load for over-reinforced sections increased by 97% as compared with balanced section and ACI 440.1R-06[9] codes showed underestimate deflection values of FRP reinforced concrete beams. Maranan et al. [12] evaluated the flexural strength of geopolymer concrete beams reinforced with (GFRP) rebars; the parameters analyzed were nominal rebar diameter, ρf, and anchorage method. Based on the experimental results, the rebar diameter had no major influence on the flexural efficiency of the beams and the serviceability efficiency of a beam is improved when the ρf increases. Yang et al. [13] presented the entire collapse progression in the form of crack destruction and energy degeneracy of concrete beams reinforced with (GFRP) rebars, they established that the advanced FE model developed is appropriate as a feasible and cost-effective method for perfect modeling and analysis of the destruction behavior of concrete beams reinforced with (GFRP) rebars, in particular in design-oriented parametric studies. Dong et al. [14] investigated the flexural performance of concrete beams reinforced with (FRP) rebars grouted in corrugated sheaths test results showed that the use of FRP rebars grouted in corrugated sleeves in beam tension zone was an active method to reduce crack sizes and improving performance in serviceability, and Reinforced FRP beams at the start of concrete crushing showed greater deflection than the steel-RC beam. FRP reinforced beams may also give a sign of catastrophe by facing significant cracking and large deflection. Ahmed et al. [15] studied Flexural strength and collapse of geopolymer simply supported concrete beams reinforced with CFRP rebars, the results showed that the ρf affected the stiffness of the beam specimens. As a result, the beams with a low ρf were significantly deformed and the final load increase (17.51–155.85 %) was verified with an increasing ρf as regards their load-deflection behavior.

There are limited studies on the behavior of continuous beams reinforced with FRP rebars, Habeeb and Ashour [16] conducted an experimental research on continuous concrete beam reinforced with (GFRP) longitudinal rebars; the major parameter investigated was the amount of GFRP reinforcement, The experimental results indicate that the over-reinforcement of the bottom layer of continuously supported GFRP beams is a main factor in monitoring the size and propagation of cracks, increasing the final load and decreasing the deflection of these kind of beams. Zinkaah and Ashour [17] experimentally tested to collapse nine continuous concrete deep beams reinforced with (GFRP) rebars, the main parameters were evaluated: the span-to-overall depth ratio of the shear, web reinforcement and the size effect, the test results were used to assess the applicability of the methods suggested by the American , European, and Canadian codes as well as previous studies to predict the load capacity of continuous deep beams reinforced with GFRP rebars. Mohamed et al. [18] examined the behavior of simple and

continuous concrete deep beams reinforced with GFRP rebars, the test parameter was the shear span-to-depth ratio, results showed that the ACI 318-14 [19] for steel-RC structures was un-conservative in calculating GFRP-RC capacity of simple and continuous beams; where the experimental load capacity was lower than the calculated ones, with an average of (0.58 and 0.74%), respectively. Abdallah et al. [20] studied the strengthening of continuous reinforced concrete (RC) beams with CFRP and GFRP rebars by using the Near Surface Mounted (NSM) technique, the major test parameters were the type, ratio and length of the FRP rebars and the filling material properties, the test results showed that the moment of redistribution and ductility of the NSM-FRP beams were adversely affected by increased FRP reinforcement, decreased FRP length or the use of mortar as a filling material rather than epoxyresin

Few available research data about the ductility of FRP reinforced members, Wang and Belarbi [21] studied the effect of fiber concrete on ductility of beams reinforced with (GFRP and CFRP) rebars, The ductility indices for all the beams tested were found to exceed the minimum requirement of 4. The adding of fibers enhanced the flexural performance by increasing the ductility level by more than (30 %). Zhu et al. [22] investigated flexural behavior of partially fiber-reinforced high-strength FRHSC beams reinforced with FRP rebars, ductility of (FR-HSC) beams reinforced with FRP rebars reduced by increasing the thickness of the (FR-HSC) layer and the fraction content of the steel fiber. For structures with high ductility requirements, it is necessary to add steel fibers at the all depth of structures.

2. Research Significance

Due to the lack of available data on the flexural behavior continuous beams reinforced with FRP rebars, this research provides a study on the behavior of this type of beams taking in consideration the increasing in concrete compressive strength and the ratio of longitudinal GFRP reinforcement also includes a study of the effect of this type of reinforcement on the catastrophe characteristics of beams like deflection, cracks width, modes of collapse and ductility and comparison the experimental results with the American , Canadian code and some proposed equations from the previous research.

3. Experimental Program

3.1 Materials

3.1.1 Concrete

The concrete mixture made of cement, fines sand, 10 mm coarse aggregates, superplasticizer, micro silica and w/c ratio, Table 1 shows the mix proportions of concrete used in this study.

Table 1. Mix proportion of concrete

Mix	G (kg/m^3)	S (kg/m^3)	C (kg/m^3)	SP %	MS (kg/m^3)	W/C
N	1000	550	400	0	0	0.45
H1	767	880	575	4	45	0.3
H2	500	900	650	4	90	0.22

G: coarse aggregate; **S**:sand; **C**:cement; MS: micro silica; **SP**:superplasticizer is % of the weight of cement; **W/C**: water-cement ratio.

3.1.2 GFRP Rebars

The used GFRP rebars in this study were produced NANJING FINGHUI ® _China [23]; rebars were contrived by the pultrusion method of E-glass fibers impregnated in modified vinyl ester resin. Table (2) provides the results of the tensile tests carried out on samples of the used GFRP rebars, tensile and modulus properties

were calculated in accordance with ASTM Standard (ASTM D7205-06) [24].

Table 2. GFRP rebars specifications

Rebar type	GFRP
Density (G/cm^3)	2.2
Final strength (MPa)	1200
Modulus of elasticity (MPa)	55000
Strain,ε_{fu} (με)	1950

3.2 Details of tested beams

The design methods defined according to the ACI 440.1R-15 [25] and ACI 318R-14 [21] were followed were followed for design nine continuous beams reinforced with GFRP rebars were divided into three groups depending on the $f'c$, Each group consists of three specimens with different GFRP ρf (ρ_{fmin}, ρ_{fb} and 1.5 ρfb), with a adequate quantity of shear reinforcement to fail either due to tensile collapse due to GFRP rebars fracturing or crushing of concrete in the central region, examined beams specifics are summed up in Table 3.

The specimens were measured with an effective range of 1100 mm for each span subjected to 2-point loading at mid of each span, all beam with rectangular section with (250×150)mm dimensions, each specimen was supported roller support assemblies and sharp edges to allow for movement and turning. Configuration of the test is outlined in Fig. 1

Table 3. Specifics of tested beams

Beam Series	Beam specimen	Beam dimensions B(mm)	Beam dimensions H(m)	Effective Span, L (mm)	Total beam length (mm)	Target concrete strength (MPa)	Bottom reinforcements (GFRP rebar's) (mm)	Top reinforcements (GFRP rebar's) (mm)	Stirrups [b]
N	BS-30-2	150	250	1100	2300	30	1φ6+2 φ10[a]	2 φ 8[a]	8@100
	BG-30-1	150	250	1100	2300	30	4φ6	2 φ 8	8@100
	BG-30-2	150	250	1100	2300	30	1φ6+2 φ10	2 φ 8	8@100
	BG-30-3	150	250	1100	2300	30	1 φ10+2φ13	2 φ 8	8@100
H1	BG-50-1	150	250	1100	2300	50	2 φ 10	2 φ 8	8@100
	B.G-50-2	150	250	1100	2300	50	3 φ 13	2 φ 8	8@100
	B G-50-3	150	250	1100	2300	50	1φ10+3 φ13	2 φ 8	8@100
H2	B G -70-1	150	250	1100	2300	70	1φ6+2 φ10	2Φ8	8@100
	B G -70-2	150	250	1100	2300	70	2 φ 16	2 φ 8	8@100
	B G -70-3	150	250	1100	2300	70	3φ16	2 φ 8	8@100

[a] reference beam reinforced with steel rebars

[b] the stirrups spacing were 100mm along the beam except interior support region were 50mm due to high shear stress

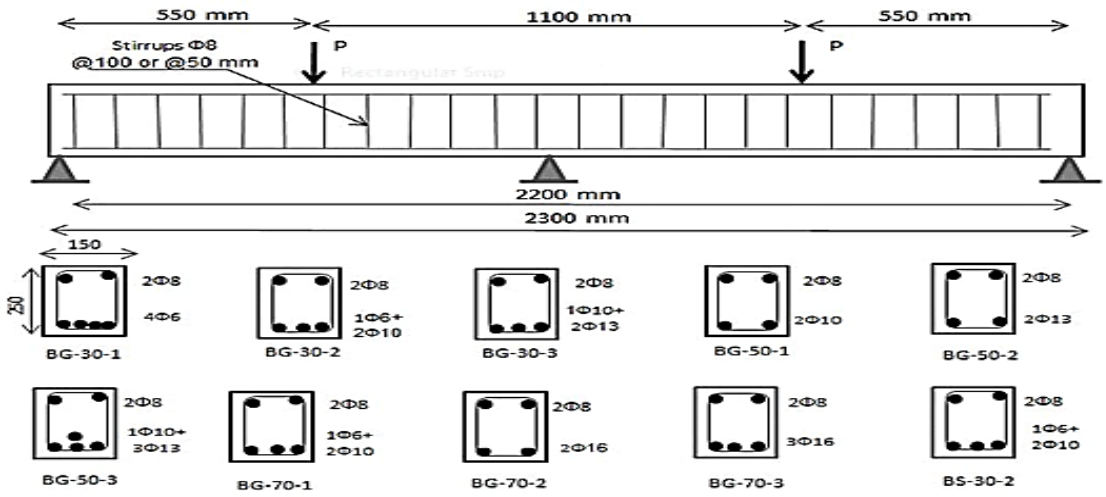

Figure 1. Tested beams geometry and details

4. Test Results and Discussion

This discussion summarizes the tests data, containing the load–deflection performance, collapse type, flexural strength, central deflection, strains concrete, GFRP strain, crack width, number of cracks and crack patterns.

4.1 Load-Deflection Performance

The experimental load of the (GFRP) reinforced concrete continuous beams to central deflection and collapse loads were shown in Figures 2 to 4. The curve matches the central beam deflection readings obtained from the dial gage. Visually examined during the test beams appear up to the first crack, and the load value corresponds was verified. The Pcr was also checked from the load- deflection figures and concrete tensile strain. Table 4 summarizes the main findings for all experiments beams**.**

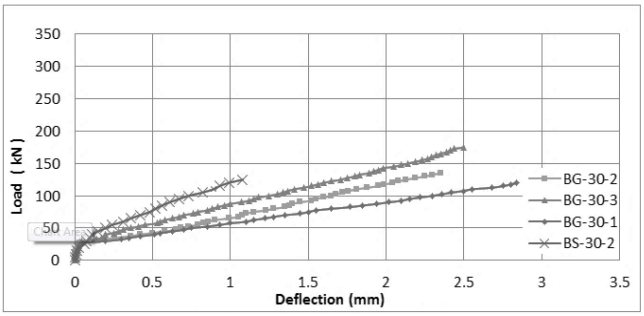

Figure 2. Load–midspan deflection of beam with fc'=30 MPa

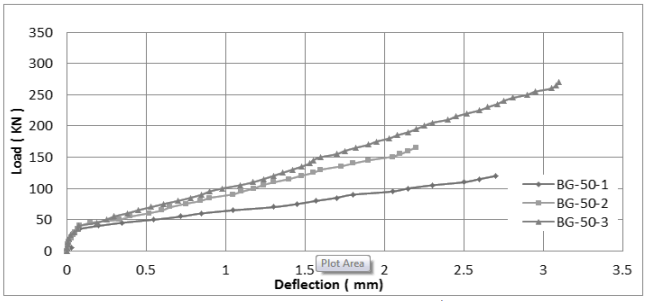

Figure 3. Load–midspan deflection of beam with fc'=50 MPa

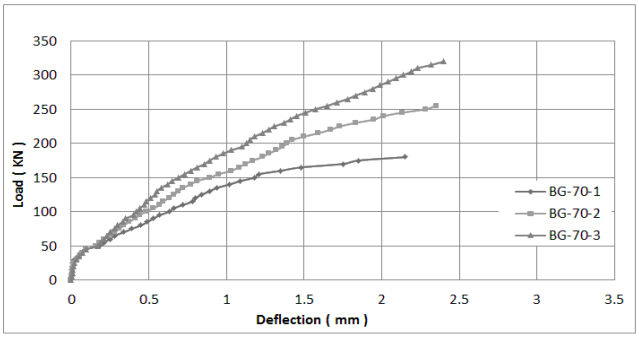

Figure 4. Load–midspan deflection of beam with fc'=70 MPa

Table 4. Experiments results and modes of collapse

Beam sample	Reinforcements Ratio (%)	$f'c$ (MPa)	Initial cracking load, P_{cr} (kN)	Collapse load, $Pu_{,exp}$ (kN)	P_{cr} / $P_{u,exp}$	Maximum midspan deflection (mm)	Collapse modes [a]
B.G-30-1	0.00383 [b]		29	119.5	0.24	2.8	G.R
B.G-30-2	0.00529 [c]	31.5	30.2	135.5	0.22	2.35	G.R+ C.C
B.G-30-3	0.00984 [d]		32	176	0.18	2.5	C.C
B.G-50-1	0.00433 [b]		38	125	0.3	2.65	G.R
B.G-50-2	0.00767 [c]	50.75	41.4	166	0.24	2.25	G.R+ C.C
B.G-50-3	0.0136 [d]		42	270	0.15	3.1	C.C
B G -70-1	0.00529 [b]		47	180	0.26	2.2	G.R
B G -70-2	0.012 [c]	71.5	48	256	0.18	2.75	G.R+ C.C
B G -70-3	0.01797 [d]		50.1	325	0.15	2.4	C.C
BS-30-2	0.00529 [e]	31.5	34.5	125	0.27	1.08	S.R

[a] C.C: crushing of concrete, G.R: GFRP rebars rupture, Steel rebars rupture.
[b] Minimum ρf (ρ_{fmin}) [c] Balanced ρf (ρ_{fb}) [d] (1.5 ρ_{fb})
[e] Reference beam reinforced by steel rebars

4.1.1 Effect of ρ_f.

Table 5 and Figure 5 illustrations the ρf influence on the collapse load, it can be gotten that the increase in (ρf) increase the collapse load, increasing the (ρf) from (ρfmin) to (ρfb) lead to increase the collapse load by (13, 38 and 42%) for beams with compressive strength (30, 50 and 70 MPa), respectively. While the increasing in collapse load when (ρf) increasing from (ρfmin) to (1.5ρfb) were (47, 125 and 80%) for the same order of f'_c ,it can be notice that the percentage of increase in collapse load was slight in normal strength concrete beams while this percentage was significant for high strength concrete beams . The increasing in (ρ_f) causing decreases the deflection at the same load level for all tested beams as shows in Figures 2 to 4.

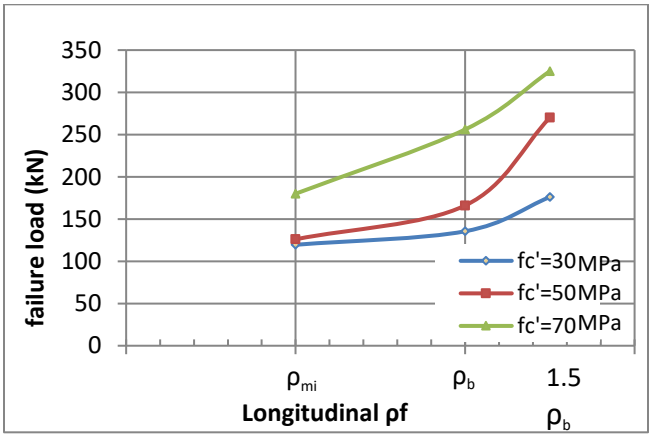

Figure5. Effect of ρf on failure loads

Table 5. Effect of ρf on collapse loads

Beam specimen	$f'c$(MPa)	Reinforcements ratio (%)	Collapse load, Pu (kN)	Increasing ratio of P_u (%)
B.G-30-1		0.383 [a]	119.5	0
B.G-30-2	31.5	0.529 [b]	135.5	13
B.G-30-3		0.984 [c]	176	47
B.G-50-1		0.433 [a]	125	0
B.G-50-2	50.75	0.767 [b]	166	38
B.G-50-3		1.36 [c]	270	125
B G -70-1		0.529 [a]	180	0
B G -70-2	71.5	0.012 [b]	256	42
B G -70-3		0.01797 [c]	325	80

[a] Minimum ρf (ρ_{fmin}) [b] Balanced ρf (ρ_{fb}) [c] (1.5 ρ_{fb})

4.1.2 Effect of concrete compressive strength

The tested specimens with the same dimensions and reinforcement area would differ only in f'_c, BG-30-2 and BG-70-1. By increasing the concrete compressive strength, the deflection in the same consequent load levels was reduced. The final load increased by 32.8% when concrete compressive strength increased from 31.5 t0 71.5 MPa. The $f'c$ had a major influence on the first crack, particularly when f'_c increased from (31.5 to 71.5 MPa), the first load of cracking increased 55.6%.

4.2 Mode of collapse.

Table 4 summarizes the modes of collapse found for the beams tested. The most common mode of collapse was concrete crushing for all over reinforced beams (beams reinforced with ($1.5\rho_{fb}$)), whereas all beams reinforced with (ρ_{fmin}) failed by rupture of GFRP rebars**.**

On the other hand the compound collapse mode (crushing of concrete and GFRP rebars rupture) was seen in all balanced reinforced sections. The ACI 440.1R-15 [25] and CSA S806-12 [26] codes recommend crushing concrete collapse for any concrete beams reinforced with FRP rebars meanwhile this type of collapse is less brittle, further gradual, and less disastrous with higher deformability related to the rupture of FRP rebars [27,28]. In addition, more shear cracks seemed and spread intensely for specimens with a higher GFRP ρf. This can be attributed to the greater shear stress relating to the higher final load. Figure 6 shows modes of collapse of the tested beams.

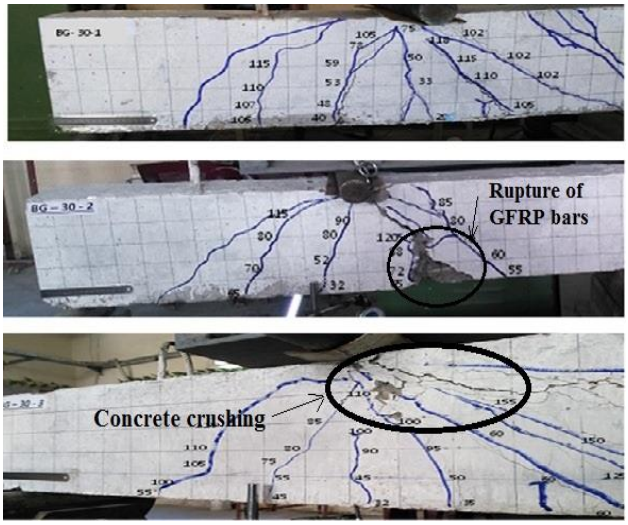

Figure 6. Collapse modes of tested beams

4.3 Load-strain relationships.

4.3.1 GFRP strain.

Figures 7 to 9 presents the load – GFRP strain relationship for all tested beams, increasing in GFRP ρf decreases the strain in rebars, at the same load level (P=119.5kN) for beams with (fc' =30) MPa the strain in the (GFRP) rebars decreased by (31 and 53%) when the ρf increased from (ρfmin) to (ρfb and 1.5 ρfb), respectively. While for beams with (fc' =50) MPa at a load of (125kN) the strain in the (GFRP) rebars decreased by (61 and 72%) as the ρf increased from (ρfmin) to (ρfb and 1.5 ρfb), respectively. In addition for beams with (fc' =70) MPa at a load of (180kN) GFRP rebars strain decreased by (57 and 78%) as the ρf increased from (ρfmin) to (ρfb and 1.5 ρfb), respectively. From the above results it can notice that the increasing in concrete compressive strength increases the decreasing percentage in GFRP rebars strain, also for beams with the same reinforcement area BG-30-2 and BG-70-1increasing the concrete compressive strength from 31.5 to 71.5 MPa decreased the GFRP strain by 32.4%.

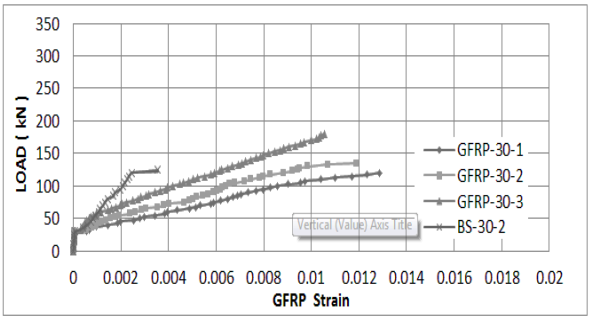

Figure 7. Load–GFRP strain of beam with $f'c$=30 MPa

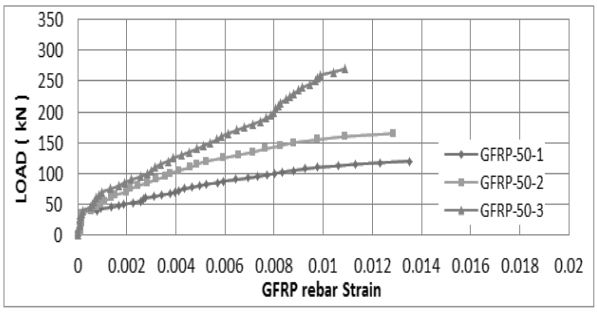

Figure 8. Load–GFRP strain of beam with $f'c$=50 MPa

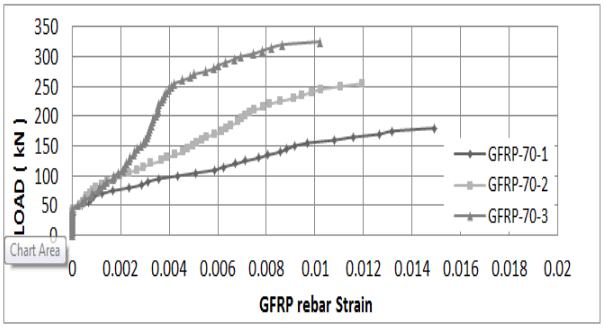

Figure 9. Load–GFRP strain of beam with $f'c$=70 MPa

4.3.2 Concrete strain

Results delivered by the two electrical strain gauges on the concrete surface at the extreme top and bottom ends of the mid-span section showed that the maximum compressive strain εcu between (0.25 and 0.33%) , these values were match with one established by the ACI440.1R-15 [25] which consider εcu to between 0.3% and 0.35%. Table 6 displays the maximum compressive and tensile strain for the experienced beams. Increasing ρf increases the final compressive strain and decreases final tensile strain for all tested beams. Table 6 showed the final compressive and tensile concrete strains.

.

Table 6. Final compressive and tensile concrete strain of tested beams

Beam sample	Reinforcements Ratio (%)	$f'c$ (MPa)	Final compresseve strain (ε_{cu})%	Final tensile strain (ε_{tu})%
BG-30-1	0.00383 [a]	31.5	0.25	1.47
BG-30-2	0.00529 [b]		0.26	1.38
BG-30-3	0.00984 [c]		0.32	1.24
BG-50-1	0.00433 [a]	50.75	0.26	1.56
BG-50-2	0.00767 [b]		0.31	1.51
BG-50-3	0.0136 [c]		0.33	1.33
BG-70-1	0.00529 [a]	71.5	0.27	1.74
BG-70-2	0.012 [b]		0.32	1.41
BG-70-3	0.01797 [c]		0.3	1.21
BS-30-2	0.00529 [d]	31.5	0.05	0.4

[a] Minimum ρf (ρ_{fmin}) [b] Balanced ρf (ρ_{fb}) [c] (1.5 ρ_{fb})
[d] Reference beam reinforced by steel rebars

4.4 Crack size

The cracks width are measured using image analyzed using Photoshop Creative Cloud (CC) software where a real scale object reference is located at the same distance of tested beam and then the captured image analyzed for crack size prediction with high accuracy. Figures 10 to 12 shows the relationship between the cracks size (Wcr) in the mid-span and the applied load on each beam, the first cracks appeared at the internal support due to the fact that the shear strength and the amount of bending moment are greater in this region than the rest of the critical sections in continuous beam.The increasing (ρf) leads to minimize the size of crack. At a load of (60 kN), the crack size noted values of, (0.43 m.m, 0.35 and 0.3 m.m) for beam (BG-30-1, BG-30-2 and BG-30-3), respectively. While, at a load of (100 kN) the size of crack is (1.3 m.m, .0.6 m.m, and 0.3 m.m) for beam (BG-50-1,

BG-50-2 and BG-50-3) respectively. In addition, at a load of (150 kN) the crack size noted values of (0.94 m.m, 0.52 m.m and 0.3 m.m) for beam (B.G-70-1, B.G-70-2and B.G-70-3), respectively, results showed that there was a significant decrease in crack size due to increasing in ρf for beams with $f'c$= 50 and 70 MPa than beams with $f'c$= 30 MPa, also for beams with the same reinforcement area BG-30-2 and BG-70-1,increasing the $f'c$ from 31.5 to 71.5 MPa decreased the crack size by 48.6%.

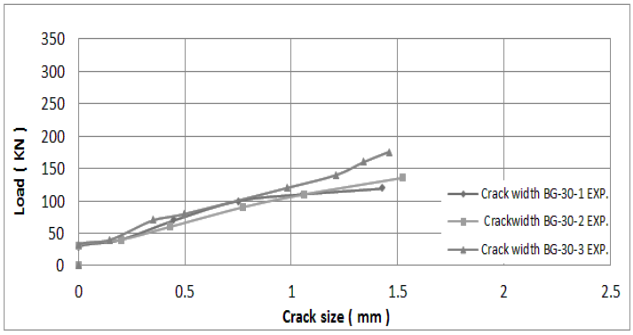

Figure 10. Load-crack size of beams with f'_c=30 MPa

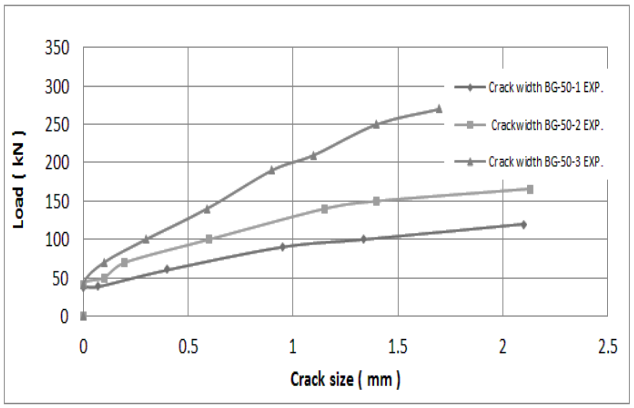

Figure 11. Load-crack size of beams with f'_c=50 MPa

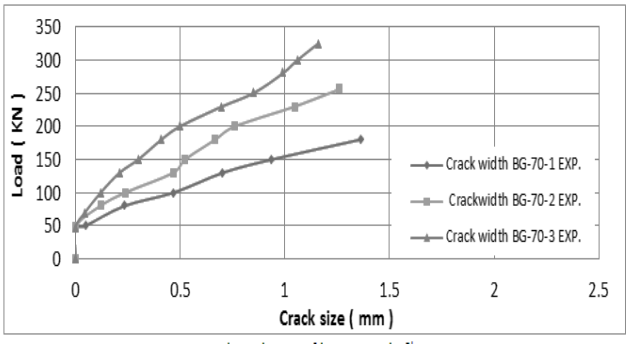

Figure 12. Load-crack size of beams with f'_c=70 MPa

The ACI 440.1R-06 [9] mentions the next formula to compute the size of crack of member reinforced by FRP rebarss :

$$W = 2\frac{f_f}{E_f}\beta K_b\sqrt{d_c^2+\frac{S^2}{4}} \qquad (1)$$

"where W is the crack size at tensile face of the beam, f_f is the stress in the FRP reinforcement, E_f is the modulus of elasticity for the FRP reinfor.cement, β is the coefficient to contrary crack size corresponding to the level of reinforcement to the tensile face of beam, kb is the coefficient that accounts for the degree of bond between the FRP rebars and the surrounding concrete, ACI 440.1R-06 [9] suggests 1.4 for deformed FRP rebars if kb is not experimentally known, dc is the thickness of concrete cover measured from extreme tension fiber to the center of the closest level of longitudinal rebars, and S is the rebars spacing. As shown in Table 3, the accurateness of evaluation is highly reliant on the value of kb, and the approximation is on the conservative side when kb = 1.4. CEB-FIP [29] model predicts the crack size as follows:

$$W = \beta S_m \varepsilon_m \qquad (2)$$

Where β = 1.3, Sm is the average crack spacing of the FRP reinforced member, ϵm is the mean reinforcement strain permitting for tension stiffening.

$$\varepsilon_m = \sigma_s[1-\beta_1\beta_2({}^{\sigma_{sr}}/_{\sigma_s})^2]/E_f \qquad (3)$$

σs is the stress in the tension reinforcement calculated on the base of a cracked section. σsr is the stress in the tension reinforcement calculated on the basis of a cracked section under loading circumstances that cause the first crack, β1= 1.0 for high-bond rebars and 0.5 for plain rebars; β2 = 1.0 for single short-term loading and 0.5 for sustained or cyclic loading.

ISIS Canada- 07[30] suggest the following equation for crack size calculation:

$$W = 2.2k_b\frac{f_f}{E_f}\frac{h_2}{h_1}\sqrt[3]{d_c A} \qquad (4)$$

Where Kb bond dependent coefficient. For FRP rebars having bond properties similar to concrete, kb=1.0, h2 distance from the extreme tension surface to the N.A., h1 distance from the centroid of tension reinforcement to the N.A. and A effective tension area of concrete surrounding the flexural tension reinforcement and having the same centroid as that reinforcement, divided by the number of rebars. Table 7 shows the experimental and calculated crack size for all tested beams.

Table 7. Experimental and calculated final crack size

Beam specimen	W_{exp} (mm)	W_{ACI} (mm)	$W_{CEB-FIP}$ (mm)	W_{ISIS} (mm)
B.G-30-1	1.43	1.28	1.38	1.43
B.G-30-2	1.52	1.4	1.49	1.55
B.G-30-3	1.46	1.34	1.55	1.45
B.G-50-1	2.1	2.35	2.17	2
B.G-50-2	2.13	2.27	2.08	1.99
B.G-50-3	1.7	1.9	1.82	1.36
B G -70-1	1.36	1.86	1.6	1.6
B G -70-2	1.26	2.17	1.85	1.5
B G -70-3	1.16	1.37	1.3	1.21

The calculations of the ACI 440 equation show lowly agreement with the test results. The accuracy of the equation mainly depends on the value of kb. Most of the test data can be enclosed between kb = 1.0 and kb = 1.4.

Following the ACI 440's recommendations, kb of 1.4 can be used to evaluation the crack size, and it is on the conservative side.

On the other hand the ISIS-Canada model's accuracy is similarly dependent on the ρf. For this study, ISIS-Canada model can calculate the crack size objectively well for the GFRP reinforced members. The cause may be: ISIS-Canada model is established based on the steel reinforced members, which usually have similar ρ_{fs} as the GFRP reinforced members in this study. While CEB-FIP equations showed good agreement with experimental results for beams having concrete compressive strength 30 and 50 MPa, but results were less consistent with the beams with strength of 70 MPa.

4.5 Comparison between GFRP and steel reinforcement.

Table 8 shows the different of experimental results of BG-30-2 and BS-30-2 were reinforced by the same rebars numbers and diameter and same concrete compressive strength but with different type of materials the first by GFRP and the second by steel rebars. Results showed that the collapse load for BG-30-2 was higher than BS-30-2 by 8.4%, while deflection, rebar's strain and crack size at collapse for BG-30-2 were higher BS-30-2 by 117.5, 240 and 740%, respectively.

Table 8. Comparison of experimental results of GFRP and steel reinforcement

Beam specimen	Pf (%)	Reinforcement type	Collapse load, Pu (kN)	Final deflection (mm)	Final strain	Final crack size (mm)
BG-30-2	0.00529	GFRP	135.5	2.35	0.0119	1.52
BS-30-2	0.00529	Steel	125	1.08	0.0035	0.18

5. Ductility

Ductility of the beam characterized as its ability to provide plastic deformation with no loss of load prior to collapse. Ductility is also indicated in terms of deformation or absorbed energy following this description. For steel rebars-reinforced elements where a strong plastic deformation of steel occurs at yield, ductility is also measured as the ratio of deformation at the final to yield. There is no yield point for reinforced FRP beams; therefore, the basic description cannot be implemented. For this reason, more than one method was proposed to calculate the ductility; the most important of these methods is shown below:

5.1 Deformability Based Approach

The deformation-based method that Jaeger et al. first introduced [31], The ductility is expressed by the deformability between the final stage and the operation stage. The force effects and the deflection effects on the ductility are taken into account. Both strength factor, (Cs), and deflection factor, (Cd) are defined as the ratio of moment or deflection values to the corresponding values at (0.001) concrete compressive stress. The strain of (0.001) is measured as the beginning of inelastic deformation of concrete [31].

$$\mu_E = C_s \times C_d \quad (5)$$

$$C_s = \frac{M_u}{M_{\varepsilon=0.001}} \quad (6)$$

$$C_d = \frac{\Delta_u}{\Delta_{\varepsilon=0.001}} \quad (7)$$

where μ_E is the ductility index.

5.2 Energy Based Approach

This approach defined Ductility as the ratio between the elastic energy absorbed and the total energy, Naaman and Jeong [32] suggested the following equation to calculate the ductility index:

$$\mu_E = \frac{1}{2}\left[\frac{E_t}{E_{el}} + 1\right] \quad (8)$$

Where Et is the total energy computed as the area under the load deflection curve, and Eel is the elastic energy computed as the area beneath line S, up to the point of intersection with $P_{collapse}$ as shown in Figure 12

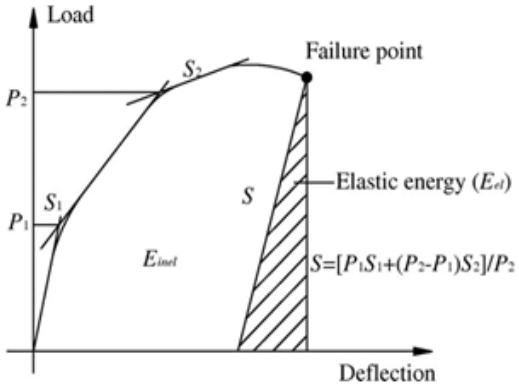

Figure 12. Energy approach definition of ductility index

The description of elastic slope depends on the selection of points P1 , P2, S1 and S2. The experimental load – deflection curves in Figures 2 to 4, however do not show any of these distinct points. The elastic slope, S, presented by Naaman and Jeong [32], is designed to quantify the elastic energy. The unloading slopes were the slope of the unloading curve corresponding to 80% of its capacity. The calculated ductility indices are summarized in Table 9.

Results showed that the ductility index by deformability approach increases with the increase of the ρf. Many FRP-beams have deformability based (μ_E) values below or close to 4 which are considered to be the minimum value for ensuring a ductile collapse as defined by CSA-S806-12 [26]. In construction of FRP reinforced beams, therefore, it is very important to test the deformability. The Jaeger [31] ductility index based on the deformation method will individually represent factors such as the

Table 9. Ductility indices by deformability and energy based approach

Beam specimen	f'_c (MPa)	Reinforcements ratio (%)	Collapse load, P_u (kN)	Deformability approach μ_E	Energy approach μ_E
B.G-30-1	31.5	0.383 [a]	119.5	2.95	2.4
B.G-30-2		0.529 [b]	135.5	3.74	1.37
B.G-30-3		0.984 [c]	176	4.9	1.23
B.G-50-1	50.75	0.433 [a]	125	2.47	1.4
B.G-50-2		0.767 [b]	166	2.68	1.19
B.G-50-3		1.36 [c]	270	5.97	1.17
B G -70-1	71.5	0.529 [a]	180	5	4.18
B G -70-2		0.012 [b]	256	7.12	3.75
B G -70-3		0.01797 [c]	325	7.4	1.27

[a] Minimum ρf (ρ_{fmin}) [b] Balanced ρf (ρ_{fb}) [c] (1.5 ρ_{fb})

load capacity. Whereas all indices of ductility determined using the Jaeger method surpassed the minimum requirements. Whereas all indices of ductility calculated using the Jaeger method surpassed minimum requirement 4 [31, 33]. On the other hand the energy approach did not provide clear and reliable results to discuss the ductility and effects of variables studied in this research on it, due to the estimation of selection points P_1, S_1, P_2 and S_2 on the load-deflection curves.

6. Conclusions

This research analyzed the flexural efficiency of continuous concrete beams reinforced with (GFRP) rebars. Evaluation of the experimental findings with the values determined using some codes equation resulted in the following conclusions within the framework of this investigation and consideration of the materials used:

1. Increasing the ρf from (ρfmin) to (ρfb), leads to increase the final capacity by (13, 38 and 42) %, for beams with $f'c$ (30, 50 and 70 Mpa), respectively. While increasing the ρf from (ρfb) to (1.5 ρfb), however, leads to increase the final ability by (30.1, and 70 Mpa), respectively.
2. The curves of load-deflection for beams with (GFRP) rebars contain three parts; the performance of the un-cracked beams reflects the first portion of the curve up to crack. The second part reflects the output of the cracked beams with reduced rigidity including a steep linear division that corresponds to the cracked beam response; and a nonlinear section after the beam.
3. Increasing the ρf shows a significant decrease in deflection at all loading stages.
4. GFRP rebars reinforced continuous beams with collapsed by crushing of concrete, meanwhile they were over-reinforced designed, whereas the under-reinforced beam failed by rupture of GFRP rebars.
5. At same load level the strain in GFRP rebars decreased with increasing in ρf, when the ρf increased from (ρfmin) to (1.5 ρfb) strain in GFRP rebars decreased by (53, 72 and 78%) for beams with $f'c$ (30, 50 and 70 Mpa), respectively.
6. The maximum compressive strain εcu between 0.25% and 0.33%, these values were match with one established by the ACI440. Increasing ρf increases the final compressive strain and decreases final tensile strain for all tested beams.

7. The cracks size was significantly decreased with increasing in ρf, at the same load level increases in ρf from (ρfmin) to (1.5 ρfb) decreasing the crack size by (30.2, 76.9 and 68%) for beams with $f'c$ (30, 50 and 70 Mpa), respectively.
8. The beam specimens with the same GFRP reinforcement area but differs only in compressive strength, BG-30-2 and BG-70-1, increasing the concrete compressive strength from 31.5 to 71.5 MPa reduced the deflection in the same consequent load levels, also first crack and final load increased by (55.6 and 32.8 %), respectively, decreased the GFRP strain and crack size by (32.4 and 48.6%), respectively and decreased number of cracks at service and final loads.
9. The effect of reinforcement type of BG-30-2 and BS-30-2 were reinforced by the same rebars numbers and diameter and same concrete compressive strength but the first reinforced by GFRP and the second by steel rebars. Results showed that the collapse load for BG-30-2 was higher than BS-30-2 by 8.4%, while deflection, rebar's strain and crack size at collapse for BG-30-2 were higher BS-30-2 by 117.5, 240 and 740%, respectively.
10. ISIS-Canada model can calculate the crack size objectively well for the GFRP reinforced members, however the calculations of the ACI 440 formula show lowly agreement with the test results.
11. The ductility index by deformability approach increases with the increase of the ρf, over-reinforced beams presents a ductile collapse where μE> 4, while beams reinforced with (ρfmin) and (ρfb) showed a brittle collapse where μE< 4 except BG-70-1, so increasing concrete compressive strength to 70 MPa change collapse type from brittle to ductile.

Conflict of interest

There are not conflicts to declare.

7. References

1. Bakis, C. E., Bank, L. C., Brown, V., Cosenza, E., Davalos, J. F., Lesko, J. J., ... & Triantafillou, T. C. (2002). Fiber-reinforced polymer composites for construction—State-of-the-art review". *Journal of composites for construction*, *6*(2), 73-87.
2. Correia, J. R., Cabral-Fonseca, S., Branco, F. A., Ferreira, J. G., Eusébio, M. I., & Rodrigues, M. P. (2006). Durability of pultruded glass-fiber-reinforced polyester profiles for structural applications. *Mechanics of Composite Materials*, *42*(4), 325-338..
3. Bai, Y., Post, N.L., Lesko, J.J. and Keller, T., 2008. Experimental investigations on temperature-dependent thermo-physical and mechanical properties of pultruded GFRP composites. Thermochimica Acta, 469(1-2), pp.28-35.
4. Fico, R. (2007). Limit states design of concrete structures reinforced with FRP bars. *University of Naples Federico II, PH. D. Thesis*..
5. Keller, T. (2001). Recent all-composite and hybrid fiber-reinforced polymer bridges and buildings. *Progress in Structural Engineering and Materials*, *3*(2), 132-140.
6. Keller, T. (1999). Towards structural forms for composite fiber materials. *Structural engineering international*, *9*(4), 297-300..
7. Sobrino, J. A., & Pulido, M. D. G. (2002). Towards advanced composite material footbridges. *Structural engineering international*, *12*(2), 84-86.

8. Barris, C., Torres, L., Turon, A., Baena, M., & Catalan, A. (2009). An experimental study of the flexural behaviour of GFRP RC beams and comparison with prediction models. *Composite Structures*, *91*(3), 286-295..
9. ACI 440.1 R-06.(2006). "Guide for the design and construction of structural concrete reinforced with FRP rebars". American Concrete Institute.
10. Yinghao, L., & Yong, Y. (2013). Arrangement of hybrid rebars on flexural behavior of HSC beams. *Composites Part B: Engineering*, *45*(1), 22-31..
11. Adam MA, Said M, Mahmoud AA, Shanour AS.(2015)." Analytical and experimental flexural performance of concrete beams reinforced with glass fiber reinforced polymer rebars. Constr". Build Mater;84:354–66.
12. Maranan GB, Manalo AC, Benmokrane B, Karunasena W, Mendis P.(2015). "Evaluation of the flexural strength and serviceability of geopolymer concrete beams reinforced with glass-fiber-reinforced polymer (GFRP) rebars". Engineering Structures.;101:529-41.
13. Yang WR, He XJ, Dai L.(2017)." Damage behavior of concrete beams reinforced with GFRP rebars". Composite Structures. .161:173-86.
14. Dong HL, Zhou W, Wang Z.(2019 May). Flexural performance of concrete beams reinforced with FRP rebars grouted in corrugated sleeves. Composite Structures. 1;215:49-59.
15. Ahmed HQ, Jaf DK, Yaseen SA.(2020 Jan). "Flexural strength and collapse of geopolymer concrete beams reinforced with carbon fiber-reinforced polymer rebars". Construction and Building Materials. 20;231:117185.
16. Tezuka M, Ochiai M, Tottori S, Sato R.(1995)."Experimental study on moment redistribution of continuous beams reinforced or pretensioned with fiber reinforced plastic". InRILEM PROCEEDINGS (pp. 387-387). CHAPMAN & HALL.
17. Zinkaah OH, Ashour A.(2019 Jun)." Load capacity predictions of continuous concrete deep beams reinforced with GFRP rebars". InStructures 1 (Vol. 19, pp. 449-462). Elsevier.
18. Mohamed, A. M., Mahmoud, K., & El-Salakawy, E. F. (2020). Behavior of Simply Supported and Continuous Concrete Deep Beams Reinforced with GFRP Bars. *Journal of Composites for Construction*, *24*(4), 04020032..
19. ACI 318R-14 .(2014)." Building code requirements for structural concrete (ACI 318-14) and commentary (ACI)". American Concrete Institute .1–519. Detroit.
20. Abdallah, M., Al Mahmoud, F., Khelil, A., Mercier, J., & Almassri, B. (2020). Assessment of the flexural behavior of continuous RC beams strengthening with NSM-FRP bars, Experimental and analytical study. *Composite Structures*, 112127..
21. Wang, H., & Belarbi, A. (2011). Ductility characteristics of fiber-reinforced-concrete beams reinforced with FRP rebars. *Construction and Building Materials*, *25*(5), 2391-2401..
22. Zhu, H., Cheng, S., Gao, D., Neaz, S. M., & Li, C. (2018). Flexural behavior of partially fiber-reinforced high-strength concrete beams reinforced with FRP bars. *Construction and Building Materials*, *161*, 587-597..
23. NANJING FINGHUI ® _China: producer of composite reinforcing elements for design and construction. China.

24. ASTM, Designation: D 7205–06. Standard Test Method for Tensile Properties of Fiber Reinforced Polymer Matrix Composite Rebars,.
25. ACI 440.1R-15,(2015)." Guide for the design and construction of Concrete Reinforced with Fiber Reinforced Polymers (FRP) rebars", ACI Committee 440, American Concrete Institute, Farmington Hills, MI, USA,.
26. CSA. (2012)."Design and construction of building structures with fiber-reinforced polymers". CSA S806-12. Mississauga, Ontario, Canada: Canadian Standards Association;.
27. GangaRao, H. V., Taly, N., & Vijay, P. V. (2006). *Reinforced concrete design with FRP composites*. CRC press..
28. Kakizawa T, Ohno S, Yonewa T. Flexural behavior and energy absorption of carbon FRP reinforced concrete beams. Am Concr Inst 1993;138: 585–98.
29. CEB-FIP.(2007)." FRP reinforcement in RC structures". Fib bulletin 40. International Federation for Structural Concrete (fib).
30. ISIS, D. M. N. (2007). 3: Reinforcing Concrete Structures with Fiber Reinforced Polymers. *Intelligent Sensing for Innovative Structures Canada*, 449-458..
31. Jaeger, L. G., Mufti, A. A., & Tadros, G. (1997, October). The concept of the overall performance factor in rectangular-section reinforced concrete members. In *Proceedings of the 3rd International Symposium on Non-Metallic (FRP) Reinforcement for Concrete Structures, Sapporo, Japan* (Vol. 2, pp. 551-559)..
32. Naaman, A. E., & Jeong, S. M. (1995, August). 45 STRUCTURAL DUCTILITY OF CONCRETE BEAMS PRESTRESSED WITH FRP TENDONS. In *Non-Metallic (FRP) Reinforcement for Concrete Structures: Proceedings of the Second International RILEM Symposium* (Vol. 29, p. 379). CRC Press..
33. Code, C. C. (2006). CAN/CSA S6-06. *Canadian Standards Association, Canada*, *734*..